Journal of Physics: Conference Series

PAPER • OPEN ACCESS

Assessment of turbulence intensity estimates from floating lidar systems

To cite this article: Felix Kelberlau *et al* 2023 *J. Phys.: Conf. Ser.* **2507** 012014

Assessment of turbulence intensity estimates from floating lidar systems

Felix Kelberlau[1], **Vegar Neshaug**[1], **Anish Venu**[2]

[1]Fugro Norway AS, Havnegata 9, 7462 Trondheim, Norway
[2]DNV

E-mail: `f.kelberlau@fugro.com`

Abstract. In the pre-construction phase of offshore wind energy projects floating lidar systems (FLS) are used for wind site assessment. Their measurements of mean wind speed and direction have proven to be accurate according to existing standards. But for the assessment of turbulence intensity (TI), a widely-accepted procedure and acceptance criteria are missing. This study investigates different evaluation methods, namely linear regression analysis and the key performance indicators (KPIs) presented by the Consortium for Advancing Remote Sensing (CFARS). The assessment is based on data from an offshore trial of the Fugro SEAWATCH Wind Lidar Buoy (SWLB) against the meteorological mast and a collocated fixed profiling wind lidar at Blyth, UK. The results show that the accuracy of TI estimates from FLS can be evaluated well, when the KPIs mean bias error (MBE) and representative TI error suggested by CFARS are used. We propose best-practice acceptance thresholds of ±1% for MBE and ±1.5% for the representative TI error. The motion-compensation approach of the SWLB works well and after compensation, its TI data are similar to the data from the fixed reference lidar. The impact of lidar-specific effects is minor in the analyzed data set and near-to-zero biases are found for all measurement elevations and wind speed bins in comparison to mast data.

1. Introduction

Floating lidar systems (FLS) are frequently used for measuring wind conditions in the pre-construction phase of offshore wind energy projects. They usually offer the most cost-effective method for acquiring high quality wind data. Stage-3 rated FLSs like the Fugro SEAWATCH Wind LiDAR Buoy (SWLB) have demonstrated a great track record of measuring primary wind data like mean wind speeds and directions accurately [1].

However, for estimates of second-order statistics like turbulence intensity (TI), it is known that the influence of lidar motion leads to an overestimation of TI values from FLS compared to what fixed lidar systems would measure [2, 3, 4]. Fugro has developed a motion-compensation algorithm that effectively takes the motion out of floating lidar and hence solves the issue of motion-induced TI [3]. In addition, it is known that profiling wind lidars measure TI differently from in-situ anemometry and measurement deviations can occur [5].

What remains unsolved is the question of how to validate TI estimates from FLS. Annex L of IEC standard 61400-12-1 prescribes a comprehensive methodology for FLS classification and validation of primary wind data, but it does not account for TI data [6]. The upcoming IEC standard 61400-50-4 on the use of floating lidars for wind measurements will have an informative annex on TI that does not prescribe a validation procedure either.

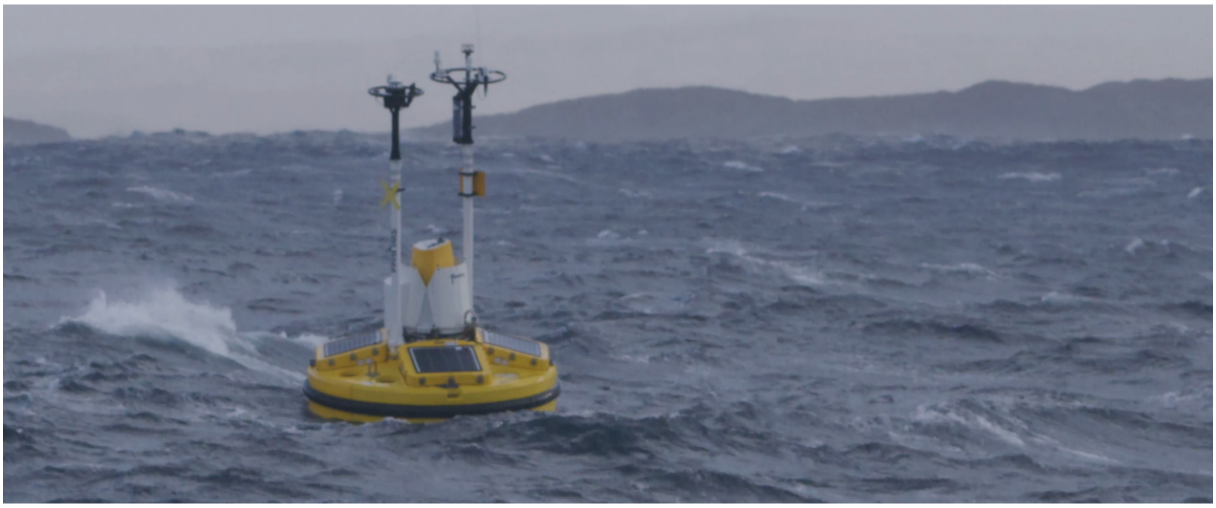

Figure 1. SEAWATCH Wind Lidar Buoy (SWLB) deployed offshore

The Carbon Trust Offshore Wind Accelerator Roadmap (Roadmap) is a widely accepted guidance document on FLS performance. It recommends to conduct linear regression analyses for comparisons of TI from FLS and trusted reference sources, but it does not provide acceptance criteria [7]. The Consortium for Advancing Remote Sensing (CFARS) issued a white paper that introduces a benchmarking framework for the assessment of TI estimates from remote sensing devices against reference values from in-situ anemometry [8]. The methodology appears well-suited also for judging the performance of a motion-compensation approach for FLS.

This study applies linear regression as recommended in the Roadmap and the CFARS evaluation scheme to data from a pre-deployment validation trial of a SWLB and reference data from the meteorological mast at Blyth. The next Section 2 describes the SWLB, the sea trial, and the methods used for the assessment of data. Section 3 thereafter presents the results of the scatter analysis and the application of the CFARS benchmark and is followed by the conclusions of the study in Section 4.

2. Methods

2.1. SEAWATCH Wind Lidar Buoy

The Stage-3 rated SEAWATCH Wind Lidar Buoy by Fugro is a FLS based on the original SEAWATCH Wavescan Buoy design (see Fig. 1). The profiling wind lidar used is the marinized version of the ZX 300 VAD-scanning continuous-wave profiling wind lidar type by ZX Lidars. For the purpose of estimating motion-compensated TI values, the buoy is equipped with a motion reference unit. Furthermore, accurate heading data is acquired by a Dual GPS system. An embedded system onboard the SWLB records the lidar line-of-sight data and calculates the required motion data in all six degrees-of-freedom. The motion-compensation algorithm is a refined version of the one previously described [3].

2.2. Blyth Test Site

The National Offshore Anemometry Hub (NOAH) at Blyth, UK, serves as reference site for the results presented here. The test site offers pairs of cup anemometers along a meteorological mast at elevations of 35m, 52m, 69m, 86m, and 103m above mean sea level. In addition, a fixed ZX300 reference lidar is collocated to the mast and measures vertical profiles of wind speeds up to 191m above mean sea level. Comparisons of FLS and reference lidar allow for benchmarking the performance of the motion compensation of the FLS. And comparisons of lidar data against cup measurements can reveal lidar-specific effects. The measurement campaign took place from Jul 23rd until Sep 9th, 2022. Flow disturbances caused by the mast are accounted for by using data from the anemometer in upwind direction only when the wind blows in boom direction (± 30 degrees). Data from the wind sector between 30 and 150 degrees are filtered because wind turbine wakes are expected. Furthermore, wind speeds below 2ms^{-1} are excluded from the assessment.

2.3. Offshore Wind Accelerator Roadmap
The Roadmap is a document that prescribes a path for FLS from the first unit built to commercial maturity. For reaching the different maturity stages, mean wind speed and direction measurements must be assessed in comparison to measurements from trusted reference sources and pass fixed acceptance criteria. TI from FLS is considered a parameter of secondary importance and the Roadmap recommends to compare TI data with values from trusted reference sources. The slope and correlation coefficient of linear regression forced through the origin are defined as the key performance indicators (KPIs) for the assessment of TI data but no acceptance criteria are given.

2.4. CFARS Benchmarking
The CFARS Site Suitability Initiative document is a guidance for the assessment of TI estimates from remote sensing devices. It suggests using the Mean Bias Error (MBE) for each 1ms^{-1}-wide wind speed bin i

$$MBE_i = \frac{1}{N_i}\sum_{n=1}^{N_i} TI_{comp,n,i} - TI_{ref,n,i} \tag{1}$$

where TI_{comp} is the comparison quantity (e.g., TI_{Lidar}), TI_{ref} is the reference quantity (e.g., TI_{Mast}), N_i is the number of values in wind speed bin i, and n is the individual data point. In addition, CFARS suggests to use the representative TI ($\mathrm{TI_{Rep}}$) error in comparisons. Representative TI is defined as the 90$^{\mathrm{th}}$ percentile of a TI distribution. Its inclusion ensures that not only the mean of all TI values but also TI variance within each wind speed bin is considered. It is calculated from $TI_{mean,i}$, the mean of all TI values in a bin and $TI_{std,i}$, its standard deviation by

$$TI_{Rep,i} = TI_{mean,i} + 1.28 TI_{std,i}. \tag{2}$$

Furthermore, the Root Mean Square Error (RMSE) shall be used to measure the TI precision. It accounts

$$RMSE_i = \sqrt{\frac{1}{N_i}\sum_{n=1}^{N_i}(TI_{comp,n,i} - TI_{ref,n,i})^2}. \tag{3}$$

3. Results
3.1. Linear regression analysis
Figure 2 shall demonstrate challenges in using ordinary linear regression for the analysis of highly scattered data. It shows TI data from the reference mast on the x-axis plotted against the same data on the y-axis. The only difference is that a temporal offset of 10 minutes is introduced, i.e., each data point consists of one TI value and its subsequent value in the time series. The resulting point cloud shows large scatter but no systematic bias. In addition to the horizontal and vertical grid lines in the background, the plot also shows diagonal grid lines that connect TI values on the y-axis with corresponding TI values on the x-axis. The x and y-values of all data pairs between two of these diagonal grid lines are averaged and plotted as red circle markers. The perpendicular distance of these diagonally-binned averages from the 1:1 line is

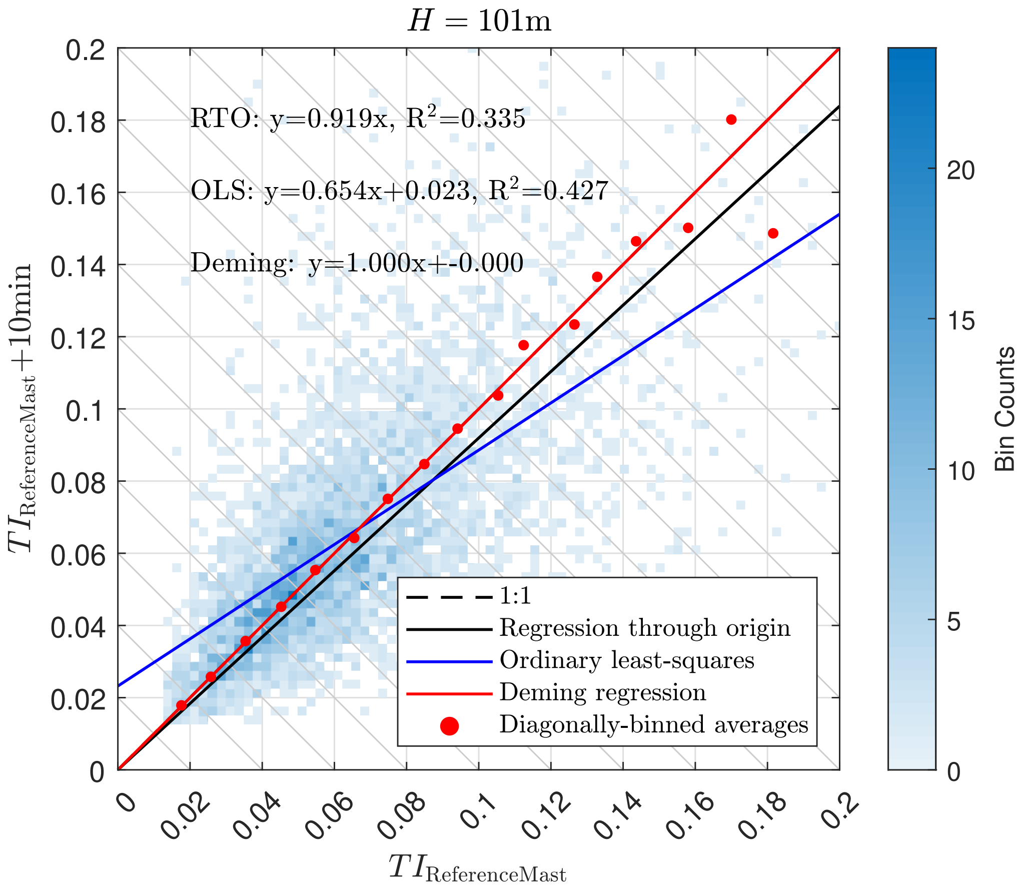

Figure 2. Scatter plot of data from reference mast on both axes with 10 minutes offset. Regression lines from linear regression through origin (black), unforced ordinary least-squares regression (blue), and Deming regression (red).

representative for the systematic bias in the data. Since the plotted data contains no bias, the diagonally-binned averages lie close to the 1:1 line for all sufficiently populated bins.

The black line in the figure is the regression line resulting from linear regression forced through the origin (RTO). This single-variant regression is often used for mean wind speed validations according to the Roadmap and is therein also recommended for TI assessments. The given example of scattered but unbiased data, shows an R^2 value below one and also the slope of the regression line is well below unity. It is important to not interpret the slope below one as a signal for bias in the data but rather as a symptom of random error or uncertainty. The result of unforced ordinary least-squares (OLS) regression shown as blue line makes this effect clearer because its slope is even lower and it has a positive offset where it meets the y-axis.

If linear regression shall be used for the analysis of systematic trends in TI scatter plots, Deming regression can be applied. The resulting regression line is shown in red and does not show any bias with a slope of one and zero offset. Deming regression assumes identical non-zero uncertainties for values on both axes and minimizes the quadratic sum of perpendicular distances of the data points from the regression line [9].

Figure 3 shows actual data from the validation trial at Blyth. Subplots (a) and (b) display motion-compensated TI data from the floating lidar system against mast reference data from 67m and 101m respectively. Subplots (c) and (d) show the floating lidar system data against the

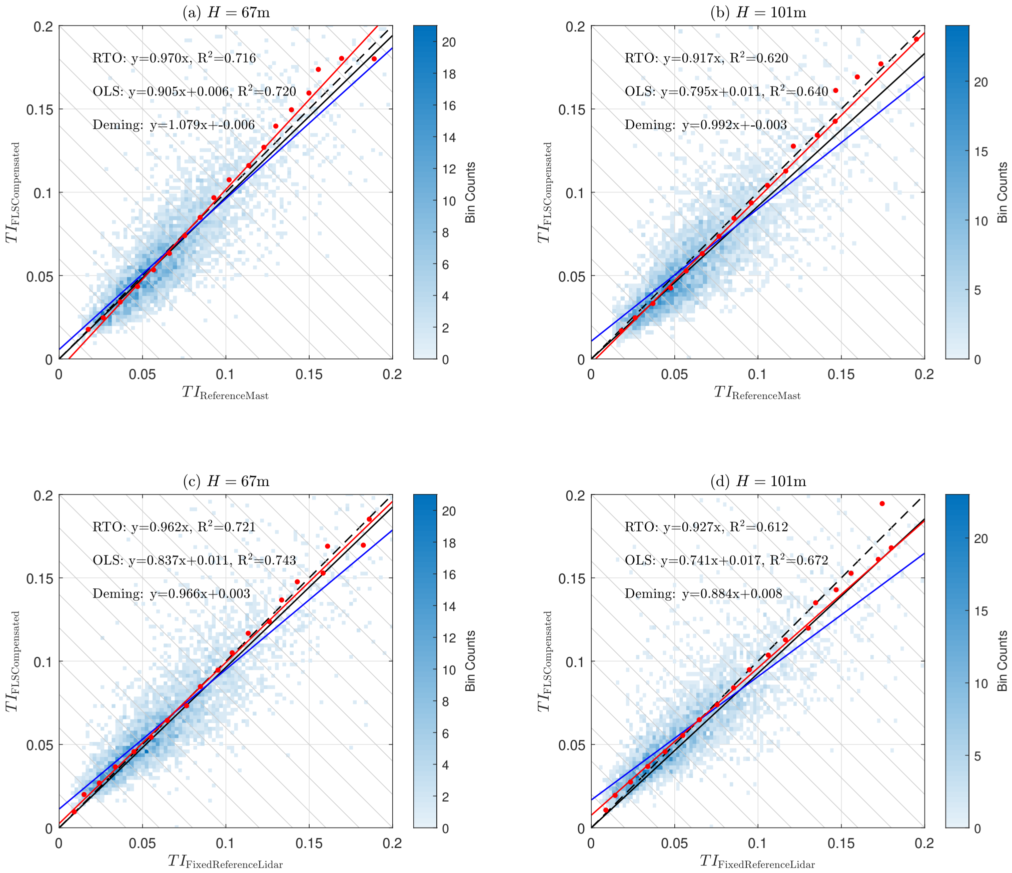

Figure 3. Scatter plot of data from floating lidar vs. reference mast (top) and fixed reference lidar (bottom) for elevations 67m (left) and 101m (right). Regression lines from linear regression through origin (black), unforced ordinary least-squares regression (blue), and Deming regression (red). Legend as in Fig. 2

fixed reference lidar for the same measurement elevations. In all four examples RTO and OLS regression shows slopes below unity and the offsets of OLS are positive like in the example of pure scatter shown in Fig. 2. Deming regression lines show slopes between 0.884 and 1.079 and offsets between -0.006 and +0.008. The diagonally-binned averages allow a more nuanced interpretation of the measurement accuracy relative to the reference TI. At 67m the FLS overestimates high TI values above 9% slightly when compared to mast data (a). But when compared to the fixed lidar this effect cannot be confirmed (c). So, this could be a lidar-specific effect. The same accounts for a small underestimation of low TI values at the same height level.

At 101m the FLS slightly underestimates medium TI values when compared to mast data (b), while it overestimates them in comparison to the fixed reference lidar (d). Systematic measurement differences between the floating lidar system and the fixed reference lidar can be caused by insufficient motion compensation. Another possible cause are the different elevations of both lidar systems above the sea. At Blyth, the fixed lidar is mounted 18m above mean sea level. When both systems scan at the same elevation above the sea, the measurement volumes and the measurement cone diameter are smaller for the fixed reference lidar. This can

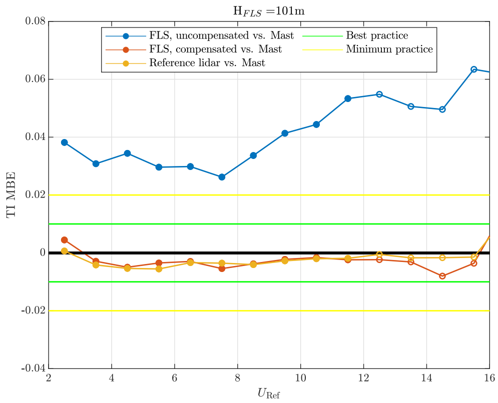

Figure 4. Mean bias error for floating lidar without (blue) and with (red) motion compensation as well as fixed reference lidar (orange) against reference mast at 101m elevation.

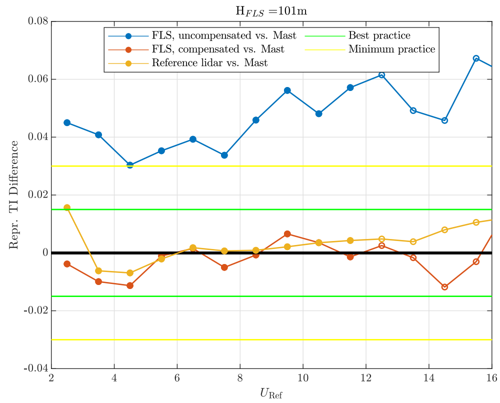

Figure 5. Representative TI error for floating lidar without (blue) and with (red) motion compensation as well as for fixed reference lidar (orange) against reference mast at 101m elevation.

introduce small measurement deviations that might influence the results presented here. Overall, systematic deviations of the SWLB data and data from the reference sources are small.

3.2. CFARS Benchmarking

An alternative to the interpretation of scatter plots, which show the measurement deviation in dependence of the reference TI, is offered in the CFARS benchmarking document. Figure 4 shows the velocity-binned mean bias errors of the uncompensated and compensated floating lidar system in blue and red respectively as well as the fixed reference lidar in orange. In all three cases mast data from 101m is the reference. The uncompensated TI data from the FLS are way too high. Especially at higher wind speeds, where they are more than 4% higher than the mast data. Uncompensated TI data from FLS should not be considered valid.

Motion-compensated TI data and the data from the fixed reference lidar show very similar MBE results for all wind speeds. The similarity of both curves shows that the motion compensation algorithm works very well in all wind speed conditions. Significant deviations are only visible for very high wind speeds above 14ms^{-1}. These high wind speed bins are sparsely populated, which is indicated by unfilled markers in the plot.

Only at very low wind speeds the lidar-measured TI is slightly higher than the corresponding values from the mast. At all other wind speeds, both lidar systems underestimate the mast TI slightly. It appears from this visualization that lidar-specific effects are small but larger than the effects of motion after compensation. All MBE values are within an error interval of $\pm 1\%$ marked as green horizontal lines in the plot.

The second suggested KPI is the representative TI error. It is shown in Fig. 5 for the same data as before. The curves for floating and fixed lidar show more variation than for MBE but the trends are the same for both. The representative TI error is close to zero and most values are within an error interval of $\pm 1.5\%$ marked as green horizontal lines. The only value outside of these bounds is the lowest wind speed bin for the fixed reference lidar. While the MBE value for this bin is close to zero, its standard deviation is too large.

The last KPI considered in this study is the RMSE shown in Fig. 6. The plot shows that the RMSE of the motion-compensated FLS is higher than the RMSE of the fixed lidar system. This is not surprising because of the larger spatial separation between the floating lidar system and the mast than between the fixed lidar and the mast. The fixed lidar might sample turbulent structures that are correlated with the turbulence measured by the mast, while the wind field sampled by the floating lidar is likely independent from what the mast samples. At least while the floating lidar and mast are not in line with the mean wind direction. Furthermore, RMSE values are higher for low wind speeds than for high wind speeds. Therefore, it appears not useful to include RMSE as a performance indicator for the assessment of TI estimates from floating lidar systems. However, it can be helpful for the comparison and evaluation of different motion compensation methodologies.

Figure 7 shows the results for MBE and TI_{Rep} error of the FLS against the reference mast for all five comparable measurement elevations. It can be seen that TI measurements from the SEAWATCH Wind Lidar Buoy after motion compensation are comparable to mast values at all heights and all wind speeds. The only elevated values are found for very low wind speeds that are not relevant for load and energy yield assessment and at very high wind speeds that were not frequent enough for statistically relevant conclusions. In many cases mast data are not available for floating lidar validation trials. Instead, fixed reference lidars are used to validate or verify the performance of floating lidar systems. Furthermore, meteorological masts offshore are often not high enough to enable comparisons of measurements taken at hub height of modern wind turbines. In these cases, the fixed lidar can be used as reference data source for TI assessments. Such comparisons allow for an assessment of the performance of the motion compensation approach but they do not discover lidar-specific effects that would be found in both, floating and fixed lidar data. Figure 8 shows the performance in terms of MBE and TI_{Rep} error of the FLS against the fixed lidar for all ten comparable measurement elevations up to 191m. For MBE, like in the comparisons against mast data, larger deviations are only found for the lowest and the highest wind speed bins. For TI_{Rep} error, a couple of outliers are found at 173m that should be investigated. The value of -2.2% at wind speeds of 8-9ms^{-1} is caused by the contribution of standard deviation of TI because its MBE is zero. The negative sign of the representative TI error means in this case that the standard deviation of the fixed lidar is higher than the standard deviation of the floating lidar. Therefore, we assume that measurement error is caused rather by the reference lidar than by the floating lidar. Finding the definite cause of this outlier requires a more detailed analysis of the underlying data. In any case, it is unlikely that the motion-compensation works worse at one particular elevation. This is supported by the averaged values in the last column of the table that show similar averaged KPI values for all elevations.

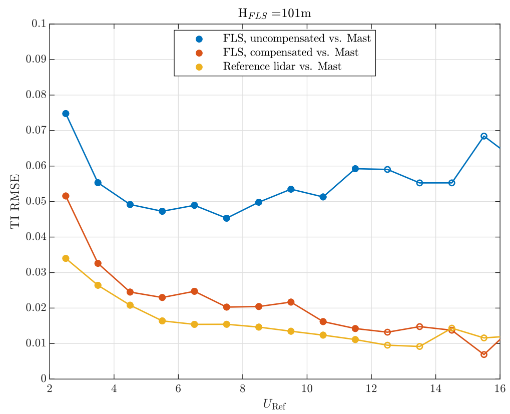

Figure 6. Root mean square error for floating lidar without (blue) and with (red) motion compensation as well as for fixed reference lidar (orange) against reference mast at 101m.

4. Conclusions

Scatter analysis can help to identify systematic trends in TI data from FLS. But we discourage from using slope and offset information from ordinary linear regression as performance indicators for measurement accuracy because both are influenced by random errors which are not entirely attributable to the FLS. Deming regression can be an alternative but should only be used if linear trends are present in the data. Non-linear correlations cannot be captured.

Adopting the CFARS TI benchmark scheme for the performance assessment of a motion-compensation approach for floating lidar systems works well and is the better option. We can demonstrate that motion-compensated TI estimates of the Fugro SEAWATCH Wind LiDAR Buoy show close-to-zero bias when compared to reference values from a meteorological mast. This accounts for both TI and representative TI values and all measurement elevations. Wind speed bins included in the assessment should be limited to the ones that are statistically and practically relevant. The random error (RMSE) is reduced to an acceptable level. Based on the measurement data presented here, we suggest the constant MBE and representative TI error thresholds listed in Table 1 for the performance assessment of FLS. For RMSE, we do not recommend to use constant thresholds for all velocity bins because comparability of RMSE values from different measurement setups is not given. Further studies of a similar kind are required to gain experience with the applied methods and to confirm that the suggested best and minimum practice criteria are suitable.

Table 1. Suggested acceptance thresholds for mean bias and representative TI benchmark

KPI	Best practice	Minimum practice
Mean bias error (MBE)	1.0%	2.0%
Representative TI error	1.5%	3.0%

Acknowledgments
We acknowledge EDF Renewables who funded the validation trial and kindly authorized publication of the results presented here.

Aggregated TI data

Mean bias error (MBE)

Height [m]	2…3	3…4	4…5	5…6	6…7	7…8	8…9	9…10	10…11	11…12	12…13	13…14	14…15	15…16	*4…16*
33	0.8 %	-0.1 %	0.0 %	-0.3 %	0.0 %	-0.2 %	-0.1 %	0.2 %	0.1 %	0.2 %	0.4 %	0.2 %	1.8 %	0.2 %	**0.2 %**
50	0.8 %	-0.2 %	-0.2 %	-0.2 %	-0.3 %	-0.2 %	-0.2 %	0.0 %	0.1 %	0.2 %	0.3 %	0.0 %	-0.4 %	-0.9 %	**-0.1 %**
67	1.3 %	0.0 %	-0.3 %	-0.3 %	-0.3 %	-0.3 %	-0.3 %	0.0 %	0.1 %	0.1 %	0.1 %	-0.1 %	-0.7 %	0.3 %	**-0.1 %**
84	1.2 %	-0.3 %	-0.4 %	-0.3 %	-0.2 %	-0.5 %	-0.3 %	0.0 %	0.0 %	-0.2 %	0.0 %	-0.2 %	-0.9 %	0.8 %	**-0.2 %**
101	0.4 %	-0.3 %	-0.5 %	-0.3 %	-0.3 %	-0.5 %	-0.4 %	-0.2 %	-0.2 %	-0.2 %	-0.2 %	-0.3 %	-0.8 %	-0.4 %	**-0.4 %**
33…101	**0.9 %**	**-0.2 %**	**-0.3 %**	**-0.3 %**	**-0.2 %**	**-0.3 %**	**-0.3 %**	**0.0 %**	**0.0 %**	**0.0 %**	**0.1 %**	**-0.1 %**	**-0.2 %**	**0.0 %**	**-0.1 %**

Representative TI error

Height [m]	2…3	3…4	4…5	5…6	6…7	7…8	8…9	9…10	10…11	11…12	12…13	13…14	14…15	15…16	*4…16*
33	0.8 %	-0.6 %	0.3 %	-0.3 %	0.2 %	-0.2 %	0.2 %	0.5 %	1.0 %	0.6 %	1.1 %	0.2 %	1.8 %	0.2 %	**0.5 %**
50	0.6 %	-0.4 %	-0.2 %	0.0 %	-0.2 %	0.1 %	0.0 %	0.4 %	0.6 %	0.8 %	0.7 %	0.5 %	-1.0 %	-0.9 %	**0.1 %**
67	1.0 %	-0.1 %	-0.3 %	-0.2 %	-0.1 %	-0.1 %	0.2 %	0.3 %	0.6 %	0.4 %	0.7 %	0.4 %	-1.0 %	0.3 %	**0.1 %**
84	1.7 %	-0.8 %	-0.8 %	-0.2 %	0.1 %	-0.3 %	0.0 %	1.0 %	0.5 %	0.1 %	0.6 %	0.0 %	-1.0 %	0.8 %	**0.1 %**
101	-0.4 %	-1.0 %	-1.1 %	-0.1 %	0.2 %	-0.5 %	-0.1 %	0.7 %	0.4 %	-0.1 %	0.3 %	-0.2 %	-1.2 %	-0.3 %	**-0.2 %**
33…101	**0.8 %**	**-0.6 %**	**-0.4 %**	**-0.2 %**	**0.0 %**	**-0.2 %**	**0.0 %**	**0.6 %**	**0.6 %**	**0.3 %**	**0.7 %**	**0.2 %**	**-0.5 %**	**0.0 %**	**0.1 %**

Figure 7. Aggregated TI data for MBE and TI_{Rep} error from the FLS with mast data as reference. Color-coding according to acceptance thresholds suggested in Table 1

Height	Aggregated TI data – Mean bias error (MBE) – Velocity bin [m/s]														
[m]	2…3	3…4	4…5	5…6	6…7	7…8	8…9	9…10	10…11	11…12	12…13	13…14	14…15	15…16	***4…16***
33	-0.9 %	-0.6 %	-0.4 %	-0.7 %	-0.6 %	-0.4 %	-0.4 %	-0.2 %	-0.2 %	-0.1 %	-0.4 %	0.3 %	0.4 %	-0.9 %	**-0.3 %**
50	0.1 %	-0.2 %	-0.2 %	-0.2 %	-0.3 %	-0.3 %	-0.2 %	-0.1 %	-0.2 %	-0.1 %	0.0 %	-0.2 %	0.3 %	-2.1 %	**-0.3 %**
67	1.2 %	0.2 %	0.1 %	-0.1 %	-0.2 %	-0.2 %	-0.1 %	0.1 %	0.0 %	-0.1 %	0.1 %	-0.1 %	-0.5 %	1.4 %	**0.0 %**
84	0.8 %	0.2 %	0.1 %	0.0 %	-0.1 %	-0.2 %	0.0 %	0.1 %	0.0 %	0.0 %	-0.1 %	-0.1 %	-0.5 %	-0.4 %	**-0.1 %**
101	0.2 %	0.4 %	0.1 %	0.0 %	0.0 %	-0.2 %	0.1 %	0.0 %	0.0 %	0.1 %	-0.1 %	-0.1 %	-0.6 %	0.0 %	**-0.1 %**
119	0.9 %	0.1 %	0.2 %	0.2 %	0.0 %	-0.2 %	0.1 %	0.0 %	0.0 %	0.0 %	0.0 %	0.3 %	-0.5 %	-0.3 %	**0.0 %**
137	1.1 %	0.3 %	0.4 %	0.2 %	0.1 %	-0.2 %	0.1 %	0.2 %	0.2 %	0.2 %	0.0 %	0.0 %	-0.1 %	0.0 %	**0.1 %**
155	0.8 %	0.2 %	0.5 %	0.2 %	0.1 %	0.0 %	0.0 %	0.2 %	0.4 %	0.2 %	0.3 %	0.1 %	-0.2 %	-0.3 %	**0.1 %**
173	0.7 %	1.1 %	0.3 %	0.4 %	0.1 %	-0.1 %	0.0 %	0.0 %	0.4 %	0.3 %	0.4 %	0.1 %	-0.3 %	-0.7 %	**0.1 %**
191	1.0 %	0.3 %	0.5 %	0.4 %	0.2 %	0.0 %	-0.2 %	0.0 %	0.2 %	0.2 %	-0.1 %	-0.3 %	-0.6 %	0.3 %	**0.0 %**
33…191	**0.6 %**	**0.2 %**	**0.1 %**	**0.0 %**	**-0.1 %**	**-0.2 %**	**-0.1 %**	**0.0 %**	**0.1 %**	**0.1 %**	**0.0 %**	**0.0 %**	**-0.3 %**	**-0.3 %**	**0.0 %**

Height	Representative TI error – Velocity bin [m/s]														
[m]	2…3	3…4	4…5	5…6	6…7	7…8	8…9	9…10	10…11	11…12	12…13	13…14	14…15	15…16	***4…16***
33	-2.9 %	-1.8 %	-1.0 %	-1.3 %	-0.8 %	-0.6 %	-0.4 %	-0.3 %	-0.3 %	0.5 %	-0.3 %	1.0 %	0.4 %	-0.9 %	**-0.3 %**
50	-1.6 %	-1.0 %	-0.7 %	-0.5 %	-0.8 %	-0.5 %	-0.2 %	-0.1 %	-0.2 %	-0.3 %	0.6 %	0.1 %	-2.6 %	-3.2 %	**-0.7 %**
67	-1.3 %	-0.4 %	-0.2 %	-0.5 %	-0.4 %	-0.6 %	0.0 %	0.1 %	-0.2 %	-0.1 %	0.1 %	-0.2 %	-0.9 %	1.4 %	**-0.1 %**
84	-2.3 %	-1.0 %	-0.8 %	-0.2 %	-0.7 %	-0.6 %	-0.1 %	0.9 %	-0.1 %	-0.1 %	-0.1 %	-0.7 %	-1.0 %	-0.8 %	**-0.4 %**
101	-3.7 %	-1.3 %	-0.5 %	-0.4 %	-0.3 %	-0.8 %	0.3 %	0.2 %	-0.1 %	0.0 %	-0.3 %	-0.6 %	-1.4 %	-0.8 %	**-0.4 %**
119	-2.3 %	-2.1 %	-0.8 %	0.0 %	-0.5 %	-0.7 %	0.2 %	0.1 %	-0.3 %	-0.1 %	-0.2 %	0.2 %	-1.6 %	-0.8 %	**-0.4 %**
137	-2.6 %	-0.5 %	-0.5 %	-0.8 %	-0.5 %	-0.9 %	0.0 %	0.1 %	0.2 %	0.4 %	-0.4 %	-0.2 %	-0.6 %	-0.4 %	**-0.3 %**
155	-2.9 %	-3.5 %	-0.7 %	-1.1 %	-0.5 %	-0.4 %	-0.3 %	-0.1 %	0.6 %	0.0 %	0.3 %	-0.3 %	-0.8 %	-1.3 %	**-0.4 %**
173	-1.6 %	0.6 %	-2.1 %	-0.1 %	-0.5 %	-0.7 %	-2.2 %	-1.2 %	0.6 %	0.4 %	0.9 %	-0.4 %	-1.0 %	-1.8 %	**-0.7 %**
191	-1.4 %	-1.8 %	-1.0 %	-0.5 %	-0.7 %	-0.1 %	-0.5 %	-0.6 %	0.1 %	-0.4 %	-0.4 %	-2.0 %	-1.8 %	0.2 %	**-0.7 %**
33…191	**-2.3 %**	**-1.3 %**	**-0.8 %**	**-0.5 %**	**-0.6 %**	**-0.6 %**	**-0.3 %**	**-0.1 %**	**0.0 %**	**0.0 %**	**0.0 %**	**-0.3 %**	**-1.1 %**	**-0.8 %**	**-0.4 %**

Figure 8. Aggregated TI data for MBE and TI_{Rep} error. Color-coding according to acceptance thresholds suggested in Table 1

References

[1] DNV GL 2021 WS181: Independent performance verification of Seawatch Wind Lidar Buoy at Frøya, Norway Tech. rep. DNV GL
[2] Gottschall J, Wolken-Möhlmann G, Viergutz T and Lange B 2014 *Energy Procedia* **53**
[3] Kelberlau F, Neshaug V, Lønseth L, Bracchi T and Mann J 2020 *Remote Sensing* **12**
[4] Salcedo-Bosch A, Farré-Guarné J, da Silva M P A and Rocadenbosch F 2023 *Remote Sensing* **15**
[5] Sathe A, Mann J, Gottschall J and Courtney M S 2011 *Journal of Atmospheric and Oceanic Technology* **28** 853–868
[6] 2017 61400-12-1:2017 edition 2.0 wind energy generation systems – power performance measurements of electricity producing wind turbines Standard International Electrotechnical Commission Geneva, CH
[7] Carbon Trust 2018 Offshore wind accelerator roadmap for the commercial acceptance of floating lidar technology Tech. rep. Carbon Trust
[8] Alexandra St Pé *et al* 2021 Site suitability initiative: An open source approach to evaluate the performance of remote sensing device (rsd) turbulence intensity measurements & accelerate industry adoption of rsds for turbine suitability assessment Tech. rep. CFARS
[9] Adcock R J 1878 *The Analyst* **5** 53–54